Stability Enhancement of an AC-AC Power Conversion Operation in Fractional Frequency Wind Energy System

Hamed Nademi, *Senior Member*, *IEEE*, and Luigi Vanfretti, *Senior Member*, *IEEE*

Department of Electrical, Computer and Systems Engineering
Rensselaer Polytechnic Institute
Troy, NY, 12180, USA

***Abstract*-Modular and scalable matrix converters are deployed in wind farms to interface the medium/high-power systems. These grids are vulnerable to instabilities during certain working conditions in addition to computational burden of existing control strategies, such as model predictive control (MPC). In this work, the operational performance of the Modular Multilevel Matrix Converter (M3C) is assessed to transmit power produced from offshore wind farm to interconnect with onshore AC grid. Small-signal impedance measurement-based stability analysis are not efficient to predict large-signal stability characteristics. The two-layer structure control design is proposed to regulate the converter branch voltages and currents. The second-layer iterative controller is embedded into an integrated perturbation analysis and sequential quadratic programming (IPA-SQP) method for handling uncertainty and overcome instability issues arise from capacitor voltage fluctuations. The complete control scheme objectives are lowering sampling time, optimization of variable constraints, and offering adaptive damping to enhance stability margin. The outcomes are verified via simulation study for a designed 9-level M3C conversion system with an equal or low operating frequency at the input or output AC grids.**

Index Terms- Modular Multilevel Matrix Converter, Model Predictive Control, Sequential Quadratic Programming, Stability Analysis, Wind power

I. INTRODUCTION

The penetration pace of renewable energy sources into the medium- or high-voltage AC and DC systems, impose huge demands of design methodologies to adhere to the existing interfaces and new grid codes. With increased complexity, interfacing guidelines intend to be deteriorated to maintain the dynamic system performance at various operating scenarios. Interoperability and dynamic interactions are well understood to be a grand challenge for the large-scale integrated power grids. For the power conversion unit to interface among different power networks, it is important to offer scalability and modularity, direct AC-AC power conversion and high quality waveforms at the output terminal. Hence, M3C topology is a promising solution in power applications providing abovementioned features. Tremendous research studies have been conducted to utilize such conversion systems in high-torque/ low-speed AC drives, low-frequency AC transmission (LFAC) networks, and offshore wind energy [1]-[3]. Common application for deploying the M3C is LFAC transmission systems, taking advantage of lesser capacitive charging current through transmission line and better fault protection [3, 4].

The key control objectives in field applications using M3C technology are [1]-[3]: (a) energy balancing and flowing circulating currents inside the converter branches, (b) operational challenges with either equal frequency at input and output AC systems or very low output frequency (1 Hz to 20 Hz), (c) regulation of converter currents at the both input and output systems, and (d) control of transferred power. Majority of different predictive-based solutions are within Model Predictive Control (MPC) category extensively adopted in multilevel power converters as addressed in [5]-[7]. Having looked into those solutions, FCS-MPC gives rather superior performance in real-time applications removing modulator and provides computational time reduction on embedded boards [6, 7].

There have been yet technical limitations to bridge the gaps on implementation of MPC solutions for the M3C [2, 8]. The available predictive strategies are heavily dependent on centralized control structures, restricting scalability feature of M3C along with the controller deficient in executing the calculations during control time interval. Distributed control concept has recently reported in [9] to improve controller performance. Although the already published solutions clearly presented progress, but most of them showing higher computational burden in real-time applications with large number of M3C cells incorporated. The phenomena of instantaneous fluctuations of cell capacitor voltages can lead to instability especially when variable speed generator is connected to the converter. Commonly used methods such as common-mode voltage injections [10] are suffering from cell voltage oscillations particularly if the generator is operated with fractional frequency. The proposed control strategy is formed to alleviate unbalanced voltages through circulating currents suppression. However, the challenge for control strategy is to tackle the induced common-mode voltage leading to offset DC in transferred branch powers when converter operates at critical frequencies; 0 Hz, 50/60Hz. As such, adaptive damping of capacitor voltage variations should be included in large part of control objectives.

The research direction here is to minimize the required switching levels in the converter while preserving an accurate M3C currents reference tracking in the input and output sides as well as bringing the voltage levels in the branches into acceptable limits based on optimization predictive methodology. In the previous publications concerning predictive techniques, integrating of optimization algorithms are also recommended to meet the required sampling time for easy implementation on embedded boards [11]-[12], however, in such algorithms the sampling time does not provide less control efforts and improved performance. In this paper, a numerical optimization algorithm called an IPA-SQP framework is expanded to tackle the common challenges related to MPC optimal control in nonlinear systems with mixed constraints on state variables and control input [13, 14]. For instance, lately in [14], the IPA-SQP formulation has been applied to direct MPC and suggested to be an effective alternative for complex systems with MMCs family conversions. In this study, the developed control scheme is applied to the high-power wind turbine generation system which is interconnected to the electrical grid via 9-level M3C configuration. Simulation analysis of the proposed controller with respect to model uncertainty in cell capacitance values, AC voltage dip and equal operating frequency for both the connected AC systems are examined.

II. TWO-LEVEL PREDICTIVE CONTROL SCHEME AND M3C CIRCUIT CONFIGURATION

A. Model of the M3C Topology

Fig. 1 presents a circuit of a (2n+1)-level M3C topology that interconnected two three-phase AC systems. As it can be seen, M3C consists of 9 branches interfacing terminals of input system ($i=a, b, c$) to the phases of output side ($j=u, v, w$). Each converter branch is formed by n-series connected H-bridge cells with an inductor. The average value of the cells capacitor voltages must be controlled with low variation and zero power mean value during steady-state operation [2]. All the capacitors will be charged up and their voltage level remain within the average value of $\sum_{i=1}^{n} v_{Capi} \Big/ n$ by the used control strategy. Here, we assume 4cells per branch, thus there are 36 cells in the entire power conversion unit. According to [2, 3] the current flowing through the converter branches, i_{branch} is described as:

$$i_{branch} = \frac{i_{si}}{3} + \frac{i_j}{3} + i_{cir} \tag{1}$$

where circulating current i_{cir} , which of two times of the output frequency relates to the capacitor voltage dynamics of each cell. By inserting inductor into branches, each branch functions as current-controlled source for suppressing the *di/dt* and the transient currents, with two times of the output frequency, appearing in branches in time instant of cells selection process [1]. The state-space equations including control input and state variables, i.e., i_{branch} and $V_c{}^h_{ij}$ are:

$$\begin{aligned} v_{branch} &= u_{si} - (L_s + \frac{L_{arm}}{3})\frac{di_{si}}{dt} - R_s i_{si} - e_j \\ &-(L_l + \frac{L_{arm}}{3})\frac{di_j}{dt} - R_l i_j - L_{arm}\frac{di_{branch}}{dt} - u_{ONe} \\ \frac{dv_{C_{ij}}{}^{h}}{dt} &= \frac{1}{C} S_i^k i_{branch} \qquad i, h = 1, \ldots n \end{aligned} \tag{2}$$

V_{branch} is the total voltage level of the all cluster cells in the converter unit. However, in our proposed control method, in which incorporates the voltage differences between neutral points of the two AC networks interconnected by M3C, the suppression of zero sequence voltage/current is achieved. Although in latest publications [10], the aforementioned voltage difference (3) is determined as common-mode voltage, yet treated as fixed coefficient unlike what is happening in practice. Additional contribution of this work related to tolerances induced capacitor voltage fluctuations and communication time-delay due to the calculation instances among controllers which are uncertainties in the optimization process. The later aspects have not been fully studied in the literature with particular focus on the current research scope of M3C.

$$|u_{ONe}| = \frac{1}{9} \sum_{\substack{i=a,b,c \\ j=u,v,w}} \sum_{\varepsilon=1}^{36} \mathrm{v}_{\varepsilon ij} \tag{3}$$

B. Two-layer Predictive Formulation with IPA-SQP Solver

In this section, the problem formulation of the proposed predictive strategy is briefly explained. The block diagram displayed in Fig. 2 shows the proposed controller for the M3C based on optimized MPC. The process of prediction states variables is segregated from the optimized variables including uncertainty and determining optimum cost function values. By integrating IPA-SQP approximations, the prediction problem is being effectively achieved, whereas the weighting coefficients are updated accordingly along with the optimal trajectories tracking for input and controlled variables produced via the first-level predictive strategy. The second-level predictive optimization scheme provides good handling uncertainty and computationally efficient alternative. The executed steps of the IPA-SQP solver including stability formulation is detailed in Fig. 3.

In [5], it is discussed that the longer prediction horizon is preferable in terms of stability aspects for control system, however, in the case of current command following of power electronics conversion, the controller horizon of one-step ahead is primarily selected. In doing so, equation (2) should be expressed in discrete domain through Midpoint Euler discretization approach presuming an input/output voltage sources remained unchanged within sampling instant T_s ($e_j(k+1) \approx e_j(k)$). Therefore, the prediction step 1 in the horizon for the necessary state variables can be derived as:

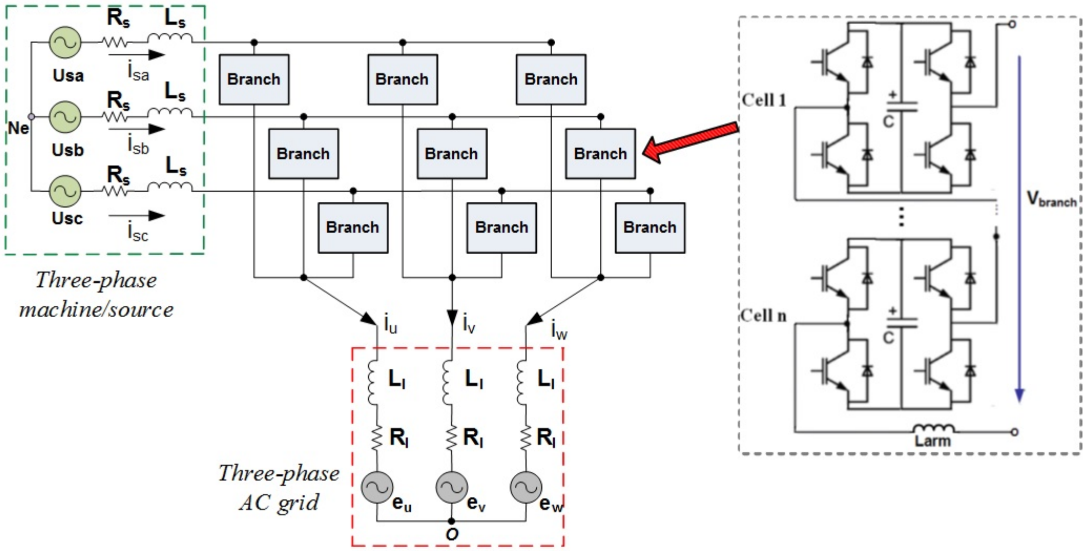

Fig. 1. Circuit diagram of a direct AC-AC M3C conversion interfaced via two different AC power systems.

$$i_{branch}(k+1) = i_{branch}(k) - \frac{T_s}{2\left(L_s + L_l + \frac{L_{arm}}{3} + T_s(R_s + R_l)\right)}.$$
$$\left[u_{si}(k) - e_j(k) - v_{branch}(k+1)\right]$$
$$v_{Cij}(k+1) = v_{Cij}(k) + S_i(k).\frac{T_s}{2C}\left(i_{branch}(k) + i_{branch}(k+1)\right) \quad (4)$$

The chosen quadratic objective function J comprising stability constraints to define the optimal switching pulses is:

$$J = \alpha_1.\left\|i^{ref}_{branch}(k+1) - i_{branch}(k+1)\right\|^2 + \alpha_2.\sum_{i=1}^{n}\left\|v_{Cij}(k+1) - V^{ref}_{Cap\_dc}\right\|^2 + \underbrace{\left|\dot{V}_{Lyapunov}\right|}_{Stability} \quad (5)$$

The optimal control sequence $u(k)$ is derived satisfying the conditional expectation and cost function tuning $J(k)$ to achieve lower computational burden. The coefficients α_1 and α_2 are computed by means of SQP numerical solver.

To address the constrained optimization of the system, as revealed in the flowchart, if at the point $x^i(t)+\delta x^i(t)$, where i is the iteration index, the Hamiltonian function (6) associated with the control state $u(t)$ is not small enough at prediction time instant k, thus the iterative procedure takes zero initial state perturbation $\delta x^i(t)=0$. More information and descriptions are given in [14, 15].

$$\sum_{k=t}^{t+N-1}\left\|H_u(k)\right\| \neq 0 \quad (6)$$

III. CASE STUDY SIMULATION RESULTS

The case-study system is developed using MATLAB/SIMULINK via 9-level M3C for analyzing purposes concerning with the proposed controller and theoretical findings. Table I gives the main circuit parameters used in the simulations. Fig. 4 presents comparative results of the obtained capacitor voltage ripples as a function of different input AC system frequency. The theoretical fluctuations for capacitor voltages derived based on the method discussed in [10]. For this analysis, the output AC grid frequency is kept constant at 50Hz.

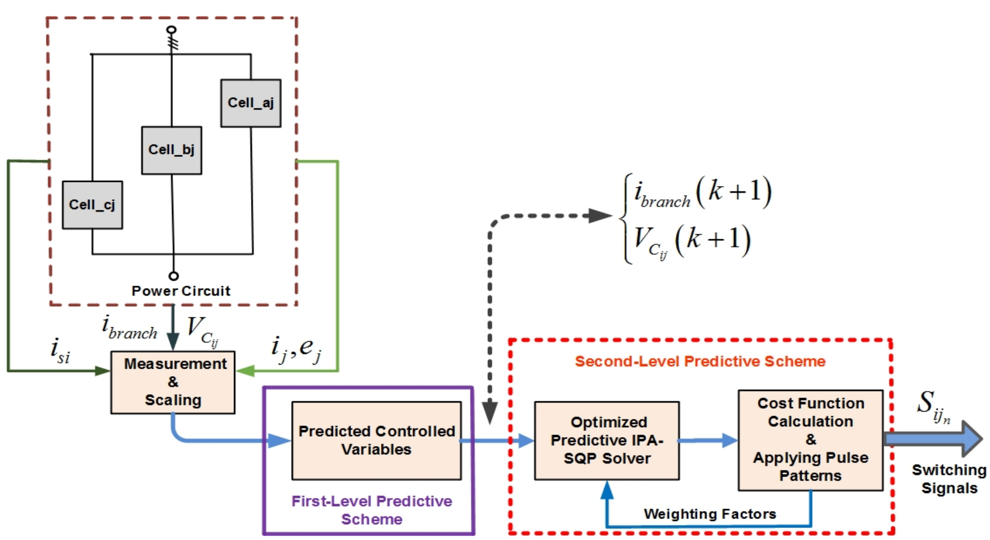

Fig. 2. Two-layer optimal predictive control structure generating the optimal switching pulses considering harmonics instability uncertainty.

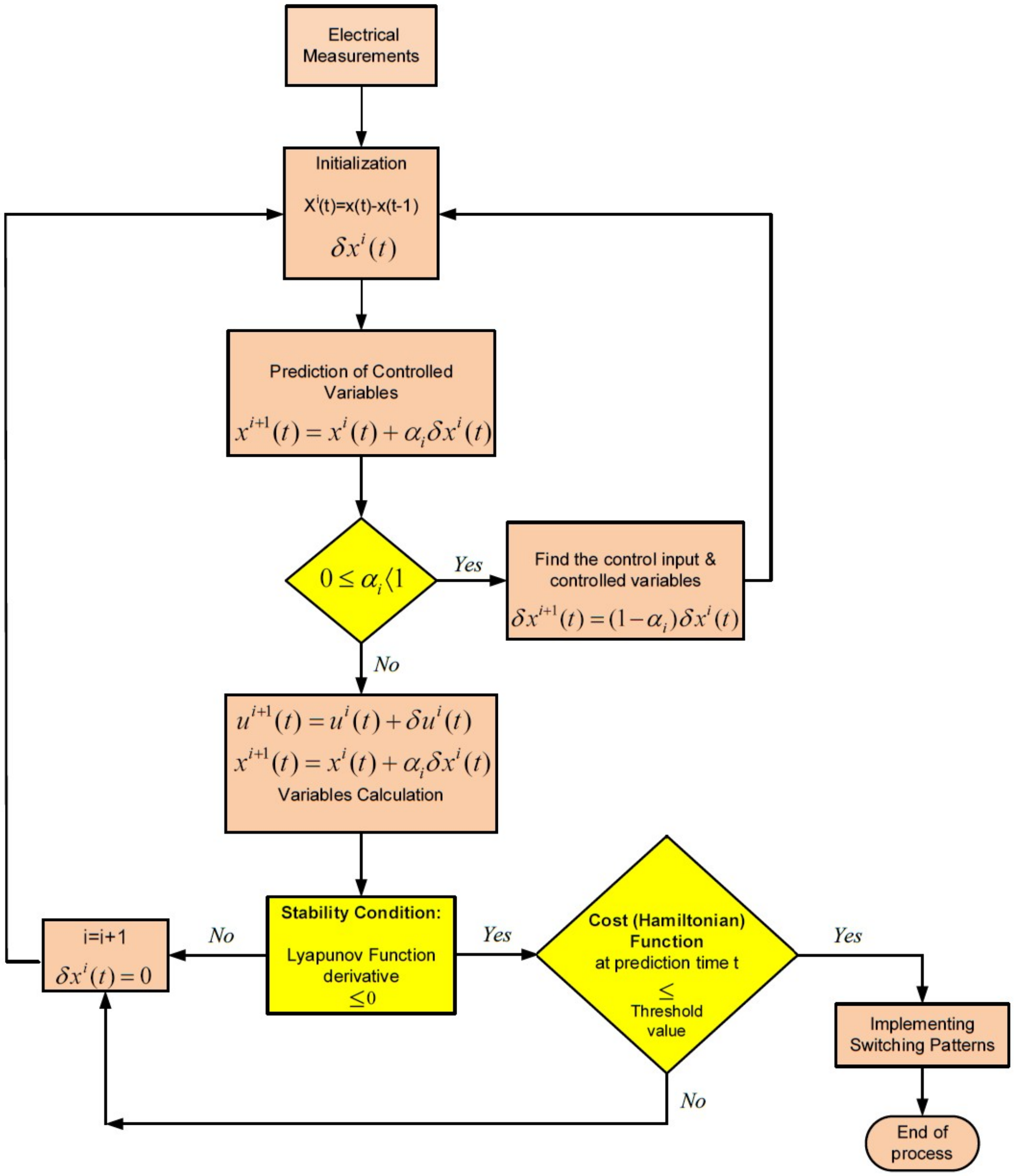

Fig. 3. Optimization strategy based on IPA-SQP applied within sampling period consisting predictive formulation and stability constraints.

The measured ripples profile among capacitor voltages obtained by the proposed control design denoting similar response within operation frequency band. It can be achieved by acceptable regulation over circulating current and common-mode voltage when converter interfaced with input/output AC systems using very low or similar operating frequency.

TABLE I. RATING PARAMETERS OF THE STUDIED SYSTEM WITH M3C

Parameters	**Value**	**Parameters**	**Value**
Full-bridge cell in each branch	4	Output system voltage	6.6kV
Input frequency	2.5-50Hz	Output system resistor	6Ω
Input system voltage	6.6kV	Output system inductor	9mH
Input system resistor	1Ω	Sampling time	30µs
Input system inductor	3mH	Branch inductance	3mH
Output frequency	50Hz	Cell capacitance	3.3mF

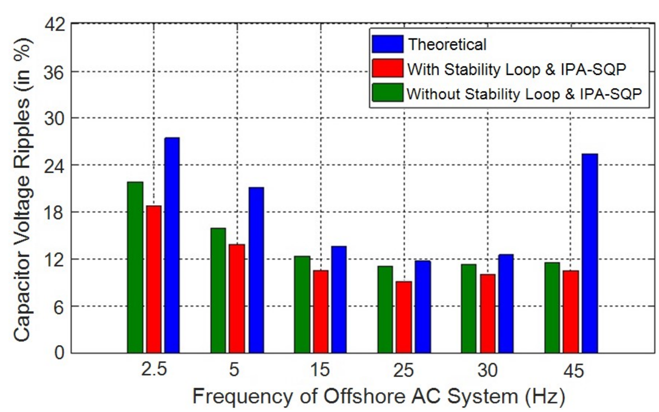

Fig. 4. Comparative results of capacitor voltage ripples at different input system frequency.

The ripples for higher frequency ranges in the operation limit demonstrate perfect match between measurements and theoretical findings. The ripple effects of cell capacitor voltages in relation with damping ratio is investigated as presented in Fig. 5.

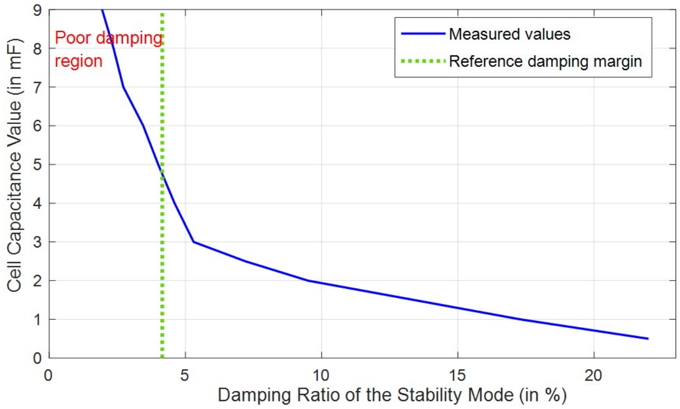

Fig. 5. Effects of cell capacitance value on the stability damping ratio due to the capacitor voltage fluctuations.

As higher capacitance values selected, poorer damping behavior is achieved negatively impact on the converter stability operation. Despite majority of existing solutions, the developed control loop accounts the stability margin associated with cell capacitor voltage ripples through assessment of predicted poor damping mode. As it is indicated in Fig. 5, in the case of cell capacitance value smaller than 5mF an acceptable damping behavior can be achieved providing an optimal way of capacitor selection in design process.

The current distortion level also satisfies the common harmonic requirements given by standards. Fig. 6 shows the branch current 1 flowing through phase's au, and branch current 2 circulates between phase av, when the input/output AC system frequency is 50/25Hz. In this operating scenario the optimization algorithm is prioritized to suppress the high-frequency harmonics only in branch current 1. Obviously, in the branch current 2, high-frequency content is still presented.

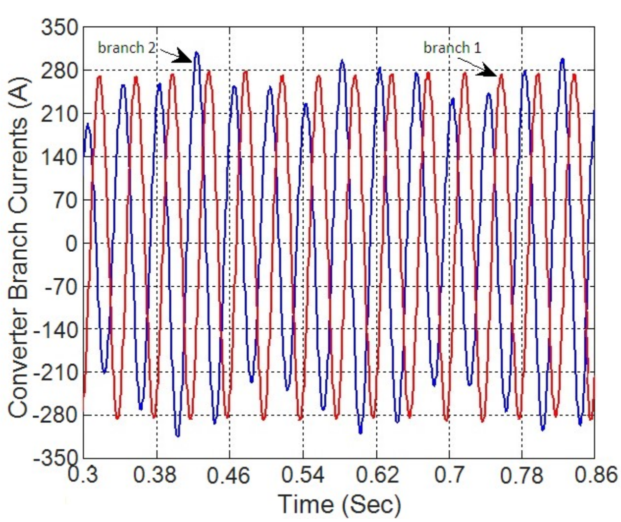

Fig. 6. High-frequency harmonics adjustment in M3C branch currents.

IV. CONCLUSION

To achieve satisfactory operation of the large-scale wind energy system, there is a need for new modeling tools with particular focus on control developments to deal with the both transients and nonlinearities appear from control loop interactions for system stability purposes. This paper has addressed an efficient two-level predictive control design for stable operation of a M3C within a wide frequency range in wind power system. This is an optimization effort in finding the cost function in each prediction horizon based on IPA-SQP solution. The most critical barriers such as common-mode voltage, nonlinearities in conversion behavior, computational burden, and damping margin due to capacitor voltage tolerances have emphasized in the proposed solution. Simulation results have confirmed functionally of the entire system with very low /equal frequency in input-output AC power supply systems over objectives, e.g., fast current command tracking, disturbance rejection properties and stability margin evaluation.

REFERENCES

[1] C. Oates, "A methodology for developing 'chainlink' converters," in *Proc. of IEEE EPE* 2009, Sept. 2009, pp. 1-10.

[2] J. Luo, X.P. Zhang, *et al.*, "Harmonic Analysis of Modular Multilevel Matrix Converter for Fractional Frequency Transmission System," *IEEE Trans. Power Del.,* vol. PP, Early Access, pp. 1-1, Oct. 2019.

[3] M. Diaz, R. Cardenas, *et al.*, "Control of Wind Energy Conversion Systems Based on the Modular Multilevel Matrix Converter," *IEEE Trans. Ind. Electron.,* vol. 64, no. 11, pp. 8799-8810, Nov. 2017.

[4] S. Liu, X. Wang, Y. Meng, *et al.*, "A Decoupled Control Strategy of Modular Multilevel Matrix Converter for Fractional Frequency Transmission System," *IEEE Trans. Power Del.,* vol. 32, no. 4, pp. 2111-2121, Aug. 2017.

[5] J. Rodriguez and P. Cortes, "Predictive Control of Power Converters and Electrical Drives," First Edition., *IEEE press-Wiley*, Mar. 2012.

[6] R. P. Aguilera, *et al.*, "Finite-Control-Set Model Predictive Control with Improved Steady-State Performance," *IEEE Trans. Ind. Informat.,* vol. 9, no. 2, pp. 658-667, May 2013.

[7] J. Rodriguez, M. P. Kazmierkowski, *et al.*, "State of the Art of Finite Control Set Model Predictive Control in Power Electronics," *IEEE Trans. Ind. Informat.,* vol. 9, no. 2, pp. 1003-1016, May 2013.

[8] A. Mora, M. Espinoza, *et al.*, "Model Predictive Control of Modular Multilevel Matrix Converter," in *Proc. of IEEE ISIE Conf.,*June 2015, pp. 1074-1079.

[9] S. Yang, Y. Tang, and P. Wang, "Distributed Control for a Modular Multilevel Converter," *IEEE Trans. Power Electron.,* vol. 33, no. 7, pp. 5578-5591, Jul. 2018.

[10] B. Fan, K. Wang, P. Wheeler, *et al.*, "A Branch Current Reallocation Based Energy Balancing Strategy for the Modular Multilevel Matrix Converter Operating Around Equal Frequency," *IEEE Trans. Power Electron.,* vol. 33, no. 2, pp. 1105-1117, Feb. 2018.

[11] P. Karamanakos, T. Geyer, N. Oikonomou, *et al.*, "Direct Model Predictive Control: A Review of Strategies That Achieve Long Prediction Intervals for Power Electronics," *IEEE Ind. Electron. Magaz.,* vol. 8, no. , pp. 32-43, Mar. 2014.

[12] Z. Yan and J. Wang, "Model Predictive Control of Nonlinear Systems With Unmodeled Dynamics Based on Feedforward and Recurrent Neural Networks," *IEEE Trans. Ind. Informat.,* vol. 8, no. 4, pp. 746-756, Nov. 2012.

[13] Y. Xie, R. Ghaemi, "Model predictive control for a full bridge DC/DC converter," *IEEE Trans. Control Syst. Technol.*, vol. 20, no. 1, pp. 164-172, Jan. 2012.

[14] H. Nademi, R. Burgos, and Z. Soghomonian "Power Quality Characteristics of a Multilevel Current Source with Optimal Predictive Scheme from More-Electric-Aircraft Perspective," *IEEE Trans. Veh. Technol.*, vol. 67, no. 1, pp. 160-170, Jan. 2018.

[15] H. Park, and J. Sun, "A tutorial overview of IPA-SQP approach for optimization of constrained nonlinear systems," in *Proc. of* 11th *WCICA*, China, Jul. 2014, pp. 1735-1740.